DARWIN fringe sensor: experimental results on the BRISE bench

Isabelle Mocœur[a,b], Frédéric Cassaing[b], Fabien Baron[c], Laurent Mugnier[b], Stephan Hofer[d] and Hans Thiele[d]

[a]Centre National d'Etudes Spatiales, France*
[b]Office National d'Etudes et de Recherches Aérospatiales, France**
[c]Cavendish Laboratory - Physics Department, United Kingdom***
[d]Kayser-Threde GmbH, Wolfratshauser Str. 48, D-81379 München, Germany

ABSTRACT

Interferometer performances are linked to the measurement and the correction of telescope aberrations. For cophasing the large number of beams required by the DARWIN mission with the specified requirements (real-time piston/tip/tilt correction and measurement of higher orders up to spherical aberration), focal-plane approach has been selected due to its simple opto-mechanical device. Several focal-plane algorithms, developed at ONERA and gathered in the stand-alone MASTIC tool, were validated by experiment with a dedicated breadboard on the laboratory test bench BRISE. Our study shows the correct behaviour of the algorithms for linearity and repeatability; specific requirements are reached for piston/tip/tilt and higher order aberrations. These results confirm the validity of focal-plane sensors for the cophasing of multiple-aperture telescopes.

Keywords: interferometry, wave-front sensing, cophasing, phase retrieval, phase diversity

1. INTRODUCTION - CONTEXT OF THE STUDY

For optical imaging instruments such as telescopes, the resolution is defined by the aperture diameter. Due to current technology and mass/volume considerations, only interferometry allows significant resolutions to be reach; the equivalent of larger diameter telescope, called MAOT for Multiple Aperture Optical Telescope, is obtained by recombination of several apertures of small diameter. In order to have the best image quality and stability at the common recombination plane, aberrations on each aperture must be corrected by a Wave-Front Sensor (WFS) with a very accurate control of the optical paths, particularly for nulling interferometers.

For DARWIN,[1] real-time piston/tip/tilt sub-nanometric correction and measurement of Higher order Aberrations (HA) with a 10 nm accuracy are required. A study for an ESA contract to Kayser-Threde and ONERA was performed to identify the best cophasing sensor for DARWIN,[2] taking into account the large number of beams (6 initially, but probably 3) and Zernike modes (1 to 11). The selected solution DWARF (DarWin AstRonomical Fringe sensor) is based on focal-plane sensing in the visible, allowing the combination of all the beams and the measurement of all the modes of interest in a single frame with a simple opto-mechanical device.

Two cophasing estimators presented Section 2 were thus developed at ONERA:

- For piston/tip/tilt, wavefront estimation is based on *Phase Retrieval* using the sole focal-plane image; retrieving sub-aperture aberrations by using intensity measurement on focal-plane was an idea first introduced by Gonsalves[3] and extended to MAOT by Paxman and Fienup.[4]
- *Phase Diversity* is based on the joint analysis of a focal and an extra-focal image which allows the measurement of higher order modes.

The breadboard DWARF was used at ONERA to validate experimentally the concept of focal-plane sensing using the laboratory test bench BRISE. We compare in Section 3 the different algorithms, presenting their performances on experimental data.

Further author information: (Send correspondence to Isabelle Mocœur)
E-mail: isabelle.mocœur@onera.fr, Telephone: +33 (0)1 46 73 47 82

2. PRESENTATION OF THE COPHASING ALGORITHMS

2.1. Formalism Problem

In this paper, we will consider multiple-aperture telescopes composed by N_T circular aperture of radius R_n. The optical transmission of the n^{th} aperture, placed at the $\boldsymbol{u_n}$ position, is written:

$$p_n = \Pi \exp(\imath \phi_n) \tag{1}$$

ϕ_n, which is the unknown aberrated phase, is expanded on a finite set of Zernike polynomials[5]:

$$\phi_n = \sum_{j=1}^{+\infty} a_{jn} Z_j(\frac{\boldsymbol{r}}{R_n}) \tag{2}$$

where a_{jn} is the amplitude of the j^{th} mode.

At the focal-plane of the multiple-aperture optical telescope, the image i observed is modelized by the noisy sampled convolution of the Point Spread Function (PSF) h with the object o:

$$i = h \star o + n \tag{3}$$

with a noise n due to measurement noise (a white noise of Gaussian distribution) and to the photon-noise which follow a Poisonnian law, but can be approximated by a Gaussian distribution at high flux.

We will introduce in Section 2.2 and 2.3 the various estimators developed for focal-plane cophasing at ONERA and gathered in the MASTIC code, the Multiple Aperture Software for Telescope Imaging and Cophasing. MASTIC can be used for simulation of the BRISE bench from both known aberrations and experimental parameters (direct model) or used for phase estimation from experimental/simulated data (inverse problem).

2.2. The Phase Retrieval

For a point source object, the acquired image is the noisy PSF h which Fourier transform, called the Optical Transfert Function (OTF), is given by:

$$h = p \otimes p = \sum_{n=1}^{N_T} \sum_{n'=1}^{N_T} (p_n \otimes p_{n'}) \star \delta_{\boldsymbol{nn'}} \tag{4}$$

The sole focal-plane image is then sufficient to reconstruct the aberrated phase coded in the pupil transmittance. For small aberrations (which is the case for real-time cophasing sensors), only the Phase Transfert Function (PTF) is affected on the first oder; phase modes appear on it as phase offsets or phase planes.[6] Thus, the OTF can be approximated as the unperturbated OTF by the PTF while effects on its modulus are neglected. With the knowledge of the global aperture configuration, all OTF peaks position are determined and coefficients from phase extracted.[7]

However, analytical algorithm was developed only for small aberrations and is not usable any more for important aberrated phase. In this case, estimation can be made by an iterative minimization of a least-square function of the unknown aberrations[8]:

$$J(\phi) = \|i - h \star o\|^2 \tag{5}$$

All necessary modes (piston and tip/tilt) for MAOT cophasing can then be determined with a single focal-plane image of a point source. We have called this concept MAESTRIA for Maximum likelihood Aberration Estimation by Short-Time phase Retrieval for Interferometric Arrays.[9] Unfortunately, single image approach are theoretically unable to retrieve unequivocally all absolute aberrations in all cases; there is a remaining sign ambiguity on the even part of the phase[10] from defocus mode.

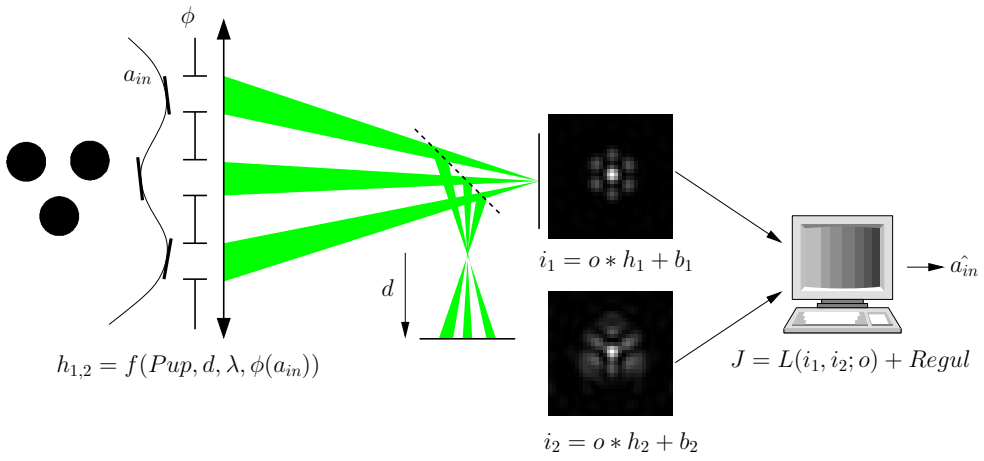

Figure 1. The phase diversity setup.

2.3. The Phase Diversity

We mentioned in Section 2.2 that Phase Retrieval from a single image generates sign ambiguity on the even part of high order aberrations. One solution to this phase retrieval problem (or, in a more general case, when observing an unknown object o) is the *Phase Diversity* (see Fig. 1), a concept first suggested by Gonsalves for as WFS for monolithic instrument.[11] This method is based on the analysis of at least two images i_1 and i_2 dephased by a known phase ϕ_d, conventionnaly a small defocus for its simple device; the images can be written as:

$$i_1 = h(\phi) \star o + n_1 \tag{6}$$
$$i_2 = h(\phi + \phi_d) \star o + n_2 \tag{7}$$

The estimation is made by minimization of the same criterion as equation 5, but applied on the two images:

$$J(o, \phi) = \|i_1 - h(\phi) \star o\|^2 + \|i_2 - h(\phi + \phi_d) \star o\|^2 \tag{8}$$

In this case, the two data sets allow to fully retrieve phase ambiguities, but with an important computation time.

3. EXPERIMENTAL RESULTS ON THE BRISE BENCH

The breadboard DWARF was used at ONERA to validate experimentally the focal-plane cophasing concept with three beams in an equilateral configuration using the ONERA laboratory test bench BRISE.[12] BRISE includes a deformable mirror composed by three planar mirrors with two of them mounted on piezo-electric platforms (called PI) which can introduce calibrated piston/tip/tilt aberrations.

3.1. Fringe Acquisition Test

First, we performed a fringe acquisition test to check that the selected algorithms have the capability to enter in the normal operation mode, *i.e.* are able to identify the central fringe during a piston acquisition. We have applied a 50 points piston-slope on the first active mirror while the opposite slope was simultaneously applied on the second one. The slopes cover all the dynamic of the PI (from 0 to 10 volts) which corresponds roughly to ± 10 μm. This test have been performed with an arc lamp and a filter of width 40 nm centred on 650 nm as described in the Section 3.2.

Figure 2 shows, for each mobile sub-aperture, the variation of visibility V. It is computed from the PSFs of the images for the baseline n-2 since the sub-aperture 2 is fixed. The visibility is defined as:

$$V = \frac{N_T I_{HF}}{I_{LF}} \tag{9}$$

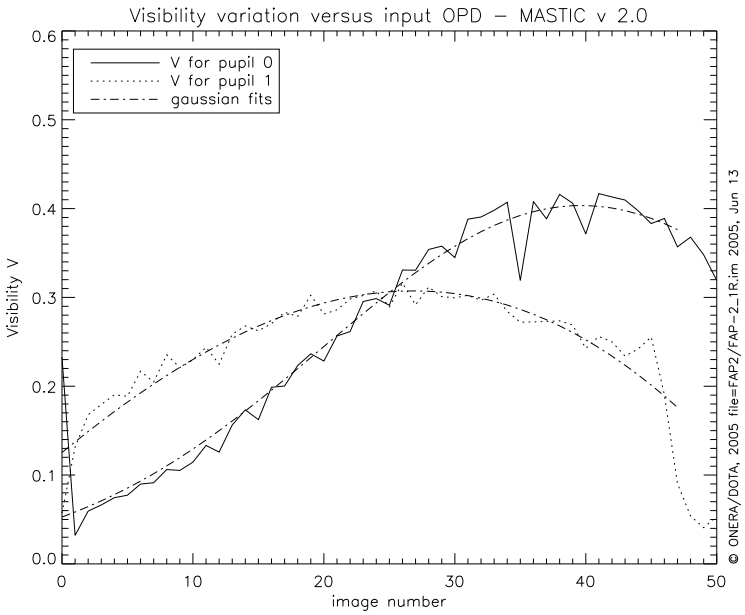

Figure 2. Visibility variation during the OPD scan.

where I_{HF} and I_{LF} are respectively the integral of the high frequency peak and of the low frequency peak of the Fourier Transform of the PSF. The graph clearly shows the variation of the fringe contrast with respect to the OPD. It also confirms that an independent information can be obtained for each baseline, thanks to the spatial encoding of the fringes. The sudden drop at the end of pupil 1 most likely comes from the fact that one of the 3 piezo has reached is maximal position whereas the other still move, creating an additional tilt. It is also possible to fit the visibility profile with a Gaussian; the fit is easy because it reduces to a least-square fit on the log of the visibility, and allows an accurate and interpolated localisation of the maximum of the visibility. DWARF has then the ability to see fringes pass over a typically 10 μm area.

3.2. Piston Measurement (Phase Retrieval)

To check the correct behaviour of the Phase Retrieval, a linearity test was first made applying a 30-point piston slope on a given sub-aperture. Because diffraction is chromatic, whereas our numerical model is monochromatic, the spectral band is one of the most important parameter to optimize. The error introduced by the width mainly consisting on a bias of the estimator, the smaller the band is, smaller the error will be. But with a small band the number of photons collected is much less important and consequently the repeatability decreases. There is thus an optimal bandwidth, resulting from a compromise between accuracy and repeatability.

Fig. 3(left) presents the piston measured by the Phase Retrieval analytic algorithm, named MAESTRIA_w, performed on different measurements using three filters of width 10 nm, 40 nm and 80 nm centred around λ_c=650 nm. Between roughly -$\lambda_c/2$ and +$\lambda_c/2$ wrapping is due to the intrinsic modulo 2π dynamic of the estimator. For small aberration, the linearity with the 10 nm and the 40 nm width filters is excellent, and piston cophasing on large spectral band (80 nm@650 nm: $\Delta\lambda = \lambda/8$) is also still possible. We also performed this test with the iterative algorithm which has shown similar results.

Fig. 3(right) presents the repeatability obtained for piston with different levels of source brightness. For each level, data set of one hundred images was acquired with the spectral filter of width 40 nm centred around 650 nm, the optimum filter considering accuracy and repeatability. For each data set, the STanDard DEViation (STDDEV) of estimated piston is plotted versus the flux N in photo-electrons.

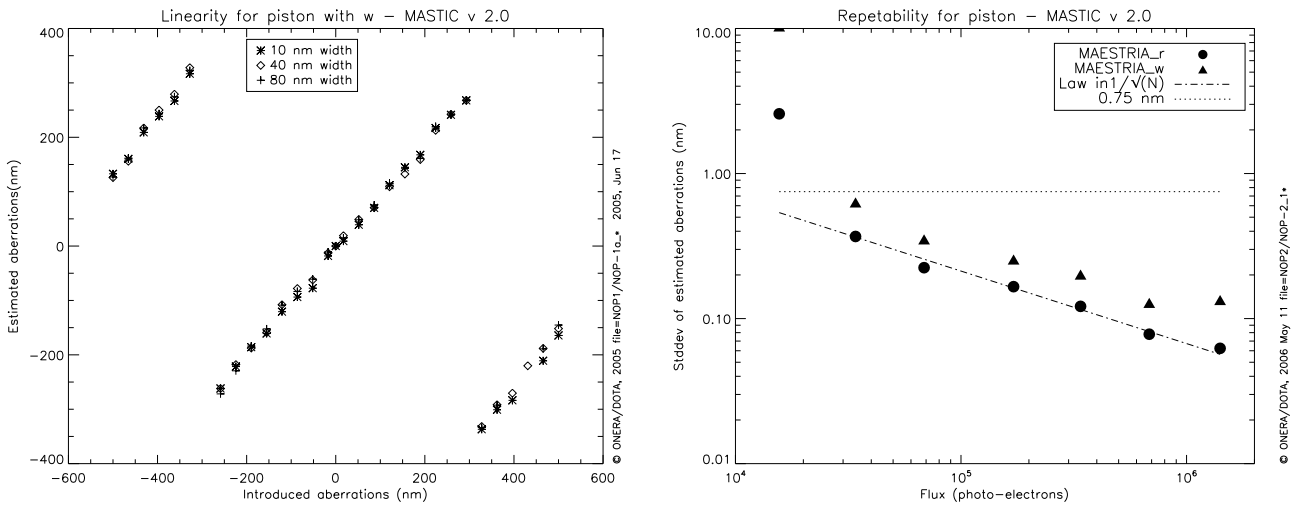

Figure 3. Piston validation using Phase Retrieval. **Left:** Estimated piston for different bandwidths with the analytic algorithm MAESTRIA_w. **Right:** Piston repeatability using the iterative (MAESTRIA_r) and the analytic algorithm.

Theoretically, the RMS error in nanometers of a cophasing algorithm is given by:

$$\sigma(\phi) = \frac{\lambda}{2\pi} \frac{\alpha}{\sqrt{N}} \tag{10}$$

We note that in photon-noise rating, estimated aberrations follow this law as expected whereas piston estimation is dominated by the detector noise at low fluxes. The iterative algorithm gives better results but piston performance is excellent in each case with a 0.75 nm repeatability specified for DWARF reached with approximatively $2\,10^4$ photo-electrons.

3.3. Tilt Measurement (Phase Retrieval)

In order to study the tilt linearity, the same tests as Section 3.2 were realized with a 30-point tilt slope. Fig. 4(right) presents the tilt estimated by MAESTRIA_w for the three spectral filters. First, we note that between $-\lambda/4$ and $+\lambda/4$, results obtained with the different filters are quite similar. Beyond $a_2 = \lambda/4$ a wrapping occurs, resulting from the fact that when $a_2 = \lambda/4$ the PSFs do not superimpose anymore; the partial slopes seen or guessed on each side of the main slope correspond to fringes created by the second ring of the tilted PSF.

Fig. 4(left) presents the standard deviation of estimated tilt with the analytical and iterative Phase Retrieval algorithms using the same data sets as Section 3.2. Aberrations follow the $1/\sqrt{N}$ law in photon-noise rating, but compared to piston performance, tilt estimations are slightly worse. However, the limiting magnitude is roughly the same for MAESTRIA_r considering the required specification. Performances are more affected using the analytical algorithm, but the magnitude is still acceptable; observations at weak flux are still allowed. In this case, the 1.21 nm repeatability specified for DWARF is reached with $1.5\,10^5$ photo-electrons.

3.4. High Orders Measurement (Phase Diversity)

We wanted to perform a similar linearity test than for piston/tip/tilt to check the correct behaviour of the high orders aberrations estimator. But when we made high order measurements, there was no HA deformable mirror mounted on BRISE. The solution we chose was to measure differential aberrations between a reference Wave Front on a planar mirror and a distorted WF made by inserting a plexy-glass plate just in front of the aperture mask; this test was performed with the spectral filter of width 40 nm centred around 650 nm. Fig. 5(left) shows the differential measurements from defocus to spherical aberration performed by the Phase Diversity algorithm on

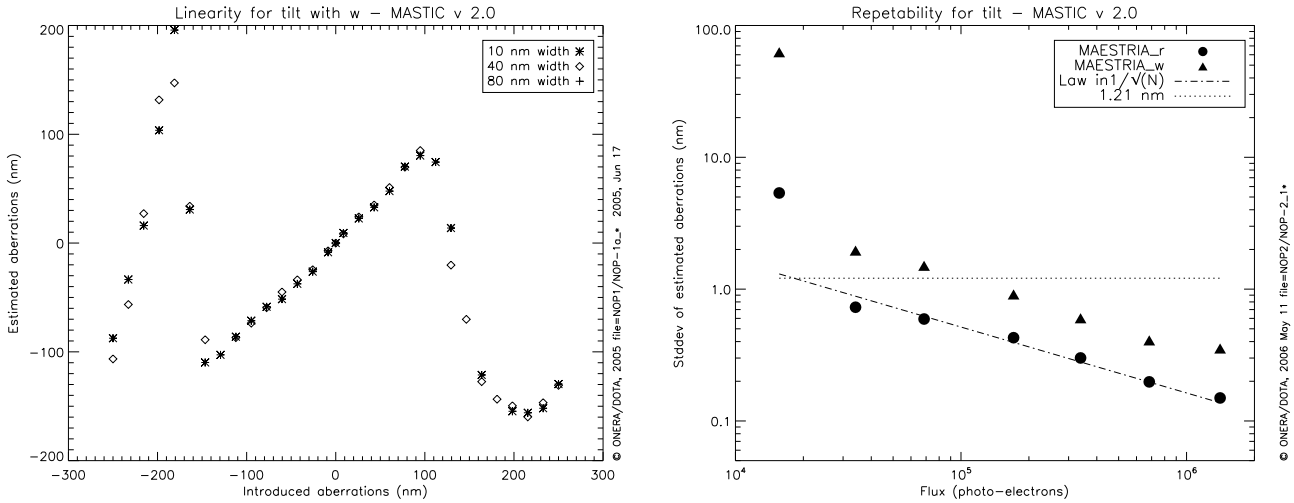

Figure 4. Tilt validation using Phase Retrieval. **Left:** Estimated tilt for different bandwidths with MAESTRIA_r. **Right:** Tilt repeatability using MAESTRIA_r and MAESTRIA_w.

DWARF and compared to ZYGO interferometer measurements. The agreement between the two measurements is quite good for the three sub-apertures. This is confirmed by the ZYGO interferogram Fig. 5(right) which shows that the apertures are dominated by astigmatism (combination of Z5 and Z6).

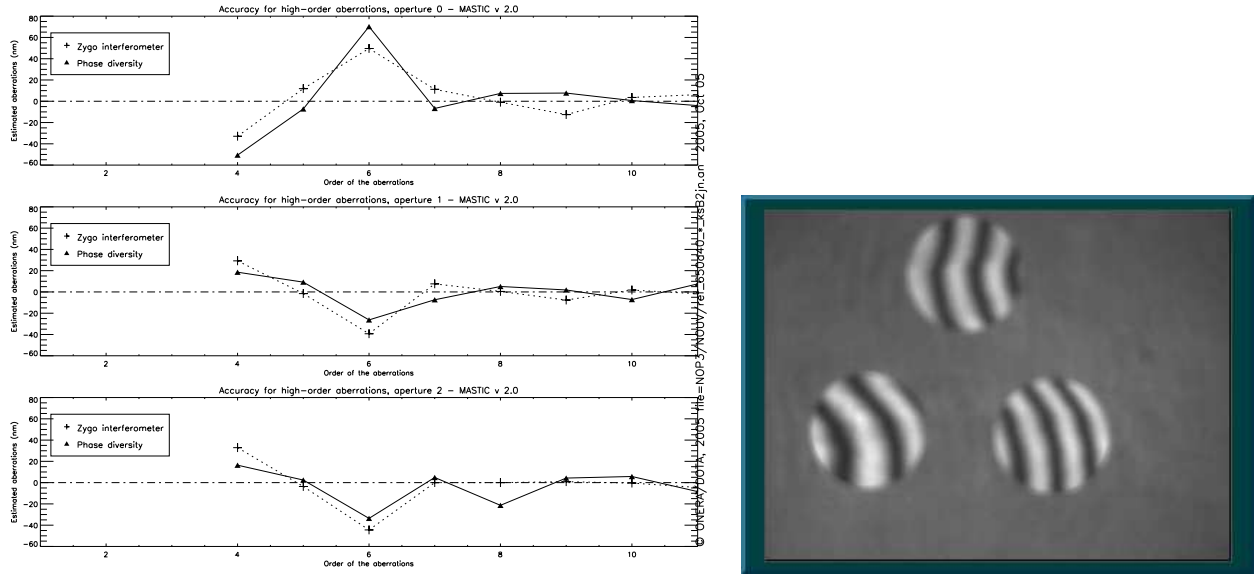

Figure 5. High orders modes linearity using Phase Diversity. **Left:** Comparison between differential hight orders measurements on DWARF and by the ZYGO interferometer. **Right:** Interferogram obtained with the ZYGO.

A repeatability test was also performed with experimental data. Even-though there was no HA deformable mirror to introduce known aberrations and check the obtained results, we used a calibrated mirror to estimate repeatability with distorted wavefronts. After piston and tip/tilt correction using the PI, we acquired 7 data sets for different flux, each composed of 70 images, and we estimated Zernike coefficients with the Phase Diversity algorithm. Figure 6 plots the standard deviation of spherical aberration (Z_{11}) versus the flux in photo-electrons.

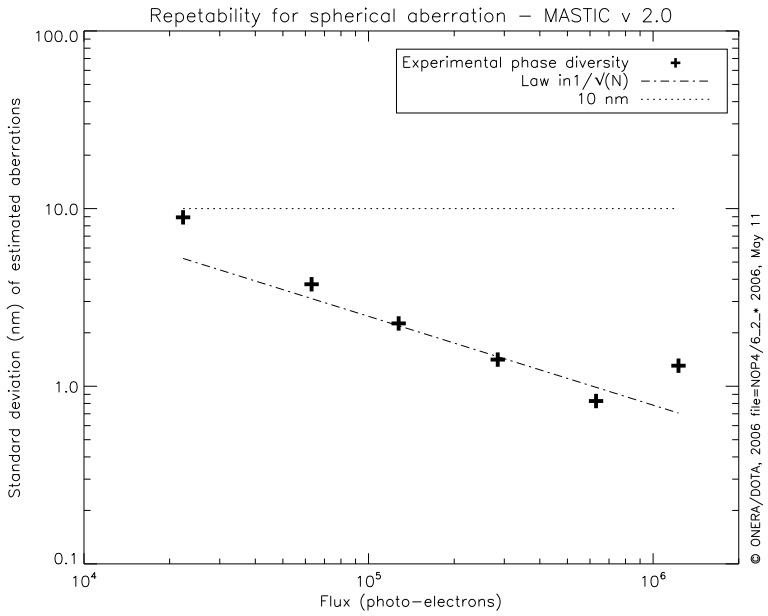

Figure 6. Repeatability for spherical aberration using Phase Diversity.

We note that estimated aberrations follow the photon-noise $1/\sqrt{N}$ law, and that the 10 nm performance is reached for about $2\,10^4$ photo-electrons, which corresponds roughly to magnitude 12.

4. CONCLUSION AND PERSPECTIVES

Nulling interferometers require a very accurate control of the optical paths. For spaceborne interferometers like DARWIN which have stringent requirements, new approachs should be considered because the classical pairwise combination leads to an unreasonable complexity. Focal-plane sensing is a promising solution, sensitive to all aberrations and which allows the measurement of all the modes of interest with little or any optics.

Two kinds of focal-plane sensors were developed at ONERA and tested on the BRISE bench: For piston/tip/tilt, real-time wavefront estimation is based on Phase Retrieval using the sole focal-plane image whereas high order aberration measurement is based on Phase Diversity. At least two images are taken, in the focal and extra-focal plane, allowing to fully retrieve the aberrated phase. Experimental results have shown that real-time piston/tip/tilt correction is possible even for limit magnitude with nanometric repeatability. Performances are also satisfying for HA modes: the use of Phase Diversity have been validated from defocus up to spherical aberration with a 10 nm accuracy. The conclusion is that focal-plane fringe-sensing is thus a simple solution which perfectly suited to DARWIN needs.

Eventhough this report has shown the very good results obtained with DWARF, which are to the best of our knowledge rather with this kind of setup, there are still some open points that deserve more investigations for a perfect understanding. We have measured the high order modes on only one point, and even if linearity performance has been validated by simulation, more complete experimental validation with a bimorph deformable mirror still remains to be done. Polychromatism can also be considered to improve accuracy and enlarge the spectral band if required.

ACKNOWLEDGMENTS

We thank DGA/SPOTI for the financial support of the BRISE developpement and ESA for supporting DWARF. We are grateful to Stephan Hofer and Hans Thiele (Kayser-Threde) for the manufacturing of the DWARF breadboard and for their fruitful discussions.

REFERENCES

1. C. Fridlhund, "The darwin mission," *Adv. in Sp. Res.* **34**(3), pp. 613–617, 2004.
2. F. Cassaing, F. Baron, E. Schmidt, S. Hofer, L. Mugnier, M. Barillot, G. Rousset, T. Stuffler, Y. Salvadé, and I. Zayer, "Darwin fringe sensor (dwarf): Concept study," in *Towards Other Earths*, **SP-539**, pp. 389–392, April 2003.
3. R. A. Gonsalves, "Phase retrieval from modulus data," *J. Opt. Soc. Am.* **66**(9), pp. 961–964, 1976.
4. R. G. Paxman and J. R. Fienup, "Optical misalignment sensing and image reconstruction using phase diversity," *J. Opt. Soc. Am. A.* **5**(6), pp. 914–923, 1988.
5. R. J. Noll, "Zernike polynomials and atmospheric turbulence," *J. Opt. Soc. Am.* **66**(3), pp. 207–211, 1976.
6. F. Cassaing, *Analyse d'un instrument à synthèse d'ouverture optique : méthodes de cophasage et imagerie à haute résolution angulaire*. PhD thesis, Université Paris XI Orsay, december 1997.
7. F. Baron, I. Mocœur, F. Cassaing, and L. Mugnier, "Cophasing of multiple-aperture telescopes from focal-plane data based on maximum likelihood methods. 1. theory and performance simulations," *J. Opt. Soc. Am. A. to be submitted* , 2006.
8. J. R. Fienup, "Phase retrieval algorithms: a comparison," *Appl. Opt.* **21**, pp. 2758–2769, aug 1982.
9. I. Mocœur, F. Baron, F. Cassaing, and L. Mugnier, "Cophasing of multiple-aperture telescopes from focal-plane data based on maximum likelihood methods. 2. simulations and experiments," *J. Opt. Soc. Am. A. to be submitted* , 2006.
10. A. Blanc, *Identification de réponse impulsionnelle et restauration d'images : apports de la diversité de phase*. PhD thesis, Université Paris XI Orsay, jul 2002.
11. R. A. Gonsalves, "Phase retrieval and diversity in adaptive optics," *Opt. Eng.* **21**(5), pp. 829–832, 1982.
12. F. Cassaing, B. Sorrente, L. Mugnier, G. Rousset, V. Michau, I. Mocœur, and F. Baron, "Brise: a multipupose bench for cophasing sensors," in *Proc. SPIE, Advances in stellar interferometry*, 2006.

* Centre National d'Etudes Spatiales - Centre Spatial de Toulouse, 18 avenue Edouard Belin, 31401 Toulouse Cedex 4, France.

** Office National d'Etudes et de Recherches Aérospatiales - Département d'Optique Théorique et Appliquée, 29 avenue de la Division Leclerc BP 72, 92322 Châtillon Cedex, France.

*** Cavendish Laboratory - Physics Department, JJ Thomson Avenue, Cambridge CB3 0HE, United Kingdom